ELSEVIER

Biochimica et Biophysica Acta 1539 (2001) 58–70

BIOCHIMICA ET BIOPHYSICA ACTA

BBA

www.bba-direct.com

Micro-Raman characterisation of the R to T state transition of haemoglobin within a single living erythrocyte

Bayden R. Wood [a], Brian Tait [b], Donald McNaughton [a,*]

[a] *Centre for Biospectroscopy and School of Chemistry, Monash University, Wellington Rd., Clayton, Vic. 3800, Australia*

[b] *Victorian Transplantation and Immunogenetics Service-Australian Red Cross Blood Services, 2nd Floor Rotary Bone Marrow Research Building, Royal Melbourne Hospital, Grattan Street, Parkville, Vic. 3052, Australia*

Received 1 August 2000; received in revised form 19 March 2001; accepted 26 March 2001

Abstract

We present the first recorded Raman spectra of haemoglobin in both the R and T states from within a single living erythrocyte using 632.8 nm excitation. Bands characteristic of low spin haems are observed in oxygenated and carboxylated erythrocytes at approx. 1636 (ν_{10}), 1562–1565 (ν_2), 1250–1245 cm^{-1} (ν_{13}) and 1226–1224 cm^{-1} ($\nu_5+\nu_8$). The spectra of deoxygenated and methaemoglobin erythrocytes have characteristic high spin bands at approx. 1610–1606 cm^{-1} (ν_{10}), 1582–1580 (ν_{37}), 1547–1544 (ν_{11}), 1230–1220 cm^{-1} (ν_{13}) and 1215–1210 cm^{-1} ($\nu_5+\nu_8$). Bands at 1172 (ν_{30}), 976 (ν_{45}) and 672 (ν_7) cm^{-1} appear to be enhanced at 632.8 nm in low spin haems. The oxidation state marker band (ν_4) at 1364–1366 cm^{-1} appeared invariant within this domain in all single cells and conditions investigated contrary to other resonance Raman studies on haem isolates. The information gained by in vivo single erythrocyte molecular analysis has important ramifications to the understanding of fundamental physiological processes and may have applications in the diagnosis and treatment of red blood cell disorders.

Keywords: Erythrocyte; Haemoglobin; Raman spectroscopy; R-T transition

1. Introduction

Early resonance Raman (RR) studies examining the out of plane translocation of the haem Fe from the porphyrin plane, thought to trigger the R (relaxed with a higher oxygen concentration) to T (tense with lower oxygen concentration) transition in haemoglobin (Hb), focussed primarily on haem isolates, haem derivatives and other model metallo-porphyrins under various physiological and non-physiological conditions [1–10]. These studies and others have utilised laser wavelengths in the vicinity of the most intense electronic transitions observed in absorption spectra of haems at about 220–200 nm (aromatic amino acid bands), 400 nm (Soret or B band) and 500–600 nm (Q_v, Q_o, or β, α bands). In addition to these bands, haem charge-transfer (CT) electronic transitions from the porphyrin to the Fe can occur in the 500–700 nm region of the electronic spectrum. A CT transition observed between 600 and 650 nm has been receiving considerable interest due to its apparent sensitivity to the haem pocket environment [11,12]. This band, which appears in the spectra of high spin ferric haem complexes, is thought to originate from a CT transition from the porphyrin to the iron $\{a'_{2u}(\pi) \rightarrow e_g(d_\pi)\}$ [12]. Salmaso et al. [13] dem-

* Corresponding author. Fax: +61-3-9905-4597;
E-mail: d.mcnaughton@sci.monash.edu.au

0167-4889/01/$ – see front matter
PII: S0167-4889(01)00089-1

onstrated that different enhancement mechanisms exist for Raman bands associated with different parts of the haem molecule by analysing the excitation profiles around the CT absorption band (623–673 nm) of eosinophil peroxidase (EPO – a high spin ferric haem). More recently, Fourier transform (FT)-Raman spectroscopy has been applied to haem isolates and human blood, revealing spectral characteristics similar to RR studies using visible excitation [14–16]. One band that has received considerable attention, due to its apparent sensitivity to electron distribution in the π-orbitals of the porphyrin macrocycle, is the band appearing between 1376 and 1355 cm^{-1}, assigned to ν_4 [17], and usually termed the oxidation state marker band. The observation that the appearance of ν_4 correlated well with haem isolates in the ferric state led to the suggestion by Yamamoto et al. [4] that the RR bands of oxygenated haemoglobin (oxyHb) supported the Weiss model [18] as to the nature of the iron-oxygen bond upon ligation [8]. In this model the oxygen molecule upon binding to deoxygenated haemoglobin (deoxyHb) withdraws an electron from the ferrous ion leaving the metal in a low spin ferric state with the oxygen converted to superoxide (O_2^-) [19]. The subsequent diamagnetism implies an anti-ferromagnetic exchange interaction between the low spin ferric ($S=1/2$) and the O_2^- ($S=1/2$) of the ligand [10]. In the high spin state the Fe is approx. 0.4 Å out of the porphyrin plane [20] and consequently the porphyrin is domed and exhibits idealised C_{4v} symmetry. In the low spin state the porphyrin is more planar and the haem exhibits an idealised D_{4h} symmetry with the inclusion of the inversion symmetry element (due to the translocation of the Fe into the plane). However, the movement of the Fe atom closer to the porphyrin plane can further distort the macrocycle reducing this planarity and increasing non-totally symmetric components. Because of its sensitivity to these porphyrin distortions resonance Raman spectroscopy has played a major part in identifying and characterising 'ruffling' effects especially in the analysis of nickel porphyrin complexes [21].

While numerous RR studies have investigated the R to T transition in isolated Hb and myoglobin (Mb), no RR (or non-resonant Raman) studies to the best of our knowledge have addressed the R to T transition in a single living red blood cell (RBC). A recent Raman confocal microspectroscopic study on single neutrophilic granulocytes demonstrated the sensitivity of the technique by distinguishing between cytochrome b_{558} and myeloperoxidase, two important enzymes in the production of intracellular bactericidal agents [22]. There has been only a brief note on the RR spectrum of isolated Hb from a single erythrocyte [23] and one paper on RR microscopy of single dehydrated erythrocytes [24].

Excitation with the 632.8 nm helium-neon (HeNe) has a number of advantageous features, compared to excitation at other wavelengths, for the analysis of single living erythrocytes. The high power needed for FT-Raman spectroscopy (100 mW–1 W) and the large numbers of scans required to produce spectra of adequate signal-to-noise would preclude analysis of living cells with 1064 nm excitation. Moreover, shorter wavelength excitation lines (≤ 514.5 nm) are known to enhance photodissociation and cause cell degradation even at low power [25].

We report for the first time Raman scattering from a single living erythrocyte recorded with a Raman microscope fitted with a water immersion objective and using the 632.8 nm excitation line generated by a HeNe laser. This configuration is applied to investigate the nature of the haem perturbation thought to initiate the R-T transition in Hb by analysing oxy and deoxy, met and carboxylated red blood cells (carboxyRBCs) in vivo.

An important question that can be addressed by this technique is whether the structural changes in the porphyrin macrocycle following deoxygenation of a single erythrocyte are similar to those reported in haem isolates and whole blood using various excitation wavelengths [1–10,14–16,26]. To corroborate band assignment we compare high spin domed porphyrins including metRBCs, deoxyRBCs, haemin, haematin with low spin planar/ruffled porphyrins including oxyRBCs, carboxyRBCs, HbA_0 and HbS. This study also reports the enhancement of vibrational modes at 632.8 nm for low spin dried oxyRBCs. An investigation into the nature of this enhancement mechanism entailed exposing samples to different excitation lines generated by a tunable dye laser (573–633 nm), a diode laser (780 nm) and a Nd:YAG laser (1064 nm).

The importance of molecular probes such as Raman microscopy to monitor Hb in the natural matrix

of an intact single cell in vivo has yet to be exploited. The techniques described in this paper may play a significant role in the understanding of the erythrocyte metabolism and could potentially be used in studies of drug design for a number of Hb disorders.

2. Methodology

2.1. Isolation and preparation of erythrocytes

Blood (10 ml) was obtained by venipuncture from healthy volunteers and placed in glass tubes containing acid citrate dextrose as an anti-coagulant. A 100 μl aliquot of blood was diluted to 10 ml with phosphate buffered saline (PBS, pH 7.4) at 4°C. Oxygen was gently bubbled into the erythrocyte solution for 10 min. The cells were washed twice, resuspended to a final volume of 10 ml in PBS saturated with O_2 and transferred to a quartz-glass petri dish (3 cm in diameter) that had been coated with a 0.01% poly-L-lysine hydrogen bromide (Sigma-Aldrich, P1274) solution and air dried. The cells were allowed to settle (approx. 10 min) and affix to the poly-L-lysine coated petri dish in a 37°C incubator. The majority of floating erythrocytes were removed by replacing the supernatant in the petri dish with fresh oxygenated PBS (4°C). To prepare deoxygenated erythrocytes a small amount of sodium dithionite ($Na_2S_2O_4$, Sigma-Aldrich, 13551) was added to the petri dish. The spectra were recorded after a 5 min incubation period at approx. 20°C. Erythrocytes were also deoxygenated by equilibrating the erythrocyte suspension with N_2. This was achieved by sealing the petri dish with a rubber cover. A hole was cut to enable positioning of the water immersion objective. N_2 gas was flowed over the top of the suspension through inlet and outlet holes bored into the rubber and positioned at opposite ends of the petri dish. N_2 is flowed at a rate of 5 cm^3/min for 60 min. CarboxyRBCs were prepared by transferring a 100 μl aliquot of deoxyRBCs to a saturated CO solution of PBS (10 ml), prepared by bubbling CO into the PBS for 30 min at approx. 20°C. The suspension was incubated for 15 min at 37°C in a sealed centrifuge tube and then transferred to a poly-L-lysine petri dish prepared as described above. MetRBCs were prepared by suspending 10 μl of packed cells into a 0.1% solution of sodium nitrite made up to 10 ml with PBS. The erythrocytes were incubated for 60 min at room temperature prior to deposition on the petri dish.

Dried oxyRBCs for excitation studies were prepared by depositing 2 μl of packed cells directly onto the KRS-5 substrate and then air dried for 60 min.

2.2. Macromolecules

Haematin (ferriprotoporphyrin hydroxide), haemin (ferriprotoporphyrin chloride), human haemoglobin A_0 (HbA_0), human haemoglobin S (HbS) and metmyoglobin (metMb) were purchased from Sigma-Aldrich. Several milligrams of each haem compound was transferred to separate 3 cm diameter quartz-glass petri dishes containing approx. 10 ml of PBS at 4°C. The crystals were allowed to settle on the bottom of the petri dish prior to spectral acquisition. Single crystals of each compound were targeted using the water immersion objective and the spectra recorded. The water immersion objective served two purposes. First, it prevented laser burning that can result from using conventional objectives in a non-aqueous environment. Second, it enabled the acquisition of spectra under the same physiological buffered conditions as the erythrocytes, thereby minimising pH effects and ensuring a valid comparison between the different haem environments. For each spectrum ten scans are accumulated with a 10 s laser exposure time. The oxidation and/or ligand states of all haem derivatives, isolates, and cells were confirmed by visible absorption spectroscopy.

2.3. Visible absorption spectroscopy

For each erythrocyte treatment mentioned above a second suspension was prepared for visible absorption spectroscopy. Cells were pelleted (2700 rpm for 2 min) and resuspended in 1.5 ml of PBS. Visible absorption spectroscopy was performed on a Cary 3 UV-Visible spectrometer in the 700–500 nm range. Spectra were baseline adjusted and vector normalised using OPUS spectroscopic software.

2.4. Raman microspectroscopy

Raman spectra of living erythrocytes were re-

corded on a Renishaw system 2000 using a 632.8 nm excitation line from a HeNe laser. The system is equipped with a modified BH2-UMA Olympus optical microscope and a Zeiss ×60 water immersion objective. Power at the sample was approx. 1.5 mW for a 1–2 μm laser spot size. Spectra were recorded between 1800 and 200 cm^{-1} with a resolution of approx. 1–2 cm^{-1}. The 520.5 cm^{-1} band of a silicon wafer is used to calibrate the instrument on a daily basis. Parallel (//) scattered light is collected by placing a half-wave plate and polariser in the light path between the sample and detector, while the perpendicular (⊥) component is collected by removing the half-wave plate. The depolarisation ratio ($p = I_{\perp}/I_{//}$) was calculated for each band, where $I_{//}$ and $I_{\perp}$ are the intensities of the parallel and perpendicular components, respectively. For each spectrum a laser exposure time of 10 s was selected and ten scans were accumulated. The laser exposure was interrupted between scans while the grating re-positioned to its starting position because constant exposure resulted in haemolysis and photodissociation. All spectra presented were interactively baseline corrected at the following points: 1800, 1687, 1494, 1282, 1200, 1027, 852, 697, 640 and 323 cm^{-1}, using the interactive algorithm in GRAMS software to enable spectral comparison. Average and standard deviation spectra were calculated using Bruker OPUS software.

Excitation spectra of dried oxyRBCs were recorded from 572 to 650 nm using a Coherent Innova 70 argon-ion laser to pump a Spectra-Physics 375B rhodamine 6G dye laser. This laser is coupled to a Dilor XY Confocal Raman Spectrometer fitted with a liquid N_2 cooled CCD. Dried erythrocytes were prepared by transferring 2 μl of packed cells (from the suspensions prepared for visible absorption spectroscopy) onto a KRS-5 substrate and air-drying for approx. 60 min. Spectra were recorded in the 1800–600 cm^{-1} domain from various spots on selected Hb crystals located around the edge of the deposit using a ×80 objective. Each spectrum is made up of eight spectral windows and the laser exposure time for each window is 180 s. Between each measurement the laser was calibrated to the 520.5 cm^{-1} silicon band and the power adjusted to approx. 1 mW. Spectra were off set corrected and normalised using Bruker OPTICS software 'make compatible' and 'vector normalisation' algorithms respectively. Spectra were smoothed using a three-point binomial smoothing algorithm (GRAMS software).

Raman spectra of crystallised HbS were collected with the Renishaw Raman confocal microscope scope fitted with the 780 nm diode laser and water immersion objective. For each spectrum ten accumulations are co-added with 10 s exposure times for each accumulation.

FT-Raman spectra were recorded on a Bruker IFS 66v FT-IR spectrometer equipped with a Bruker FRA Raman module and Nd-YAG (1064 nm) excitation source. Power at the sample is approx. 100 mW and 256 scans were co-added at a resolution of 4 cm^{-1}. The sample (approx. 200 μg of crystallised HbS) was moistened to prevent burning and tightly packed into a macrosample holder prior to spectral acquisition.

3. Results

3.1. Visible absorption spectroscopy

Fig. 1 depicts visible absorption spectra of human oxyRBCs, deoxyRBCs and metRBCs showing the position of the HeNe laser excitation line relative to the electronic transitions of the haem. The spectra

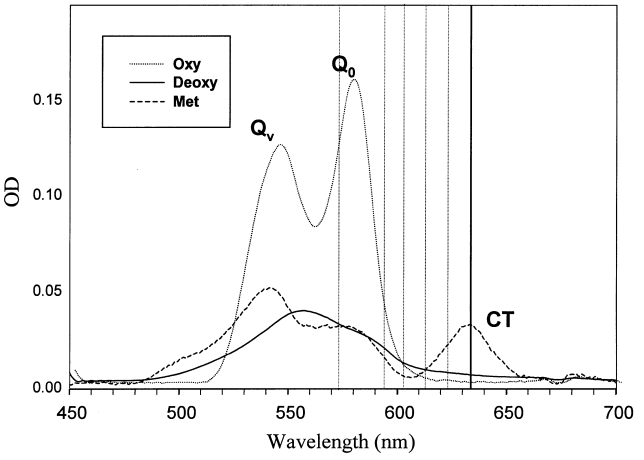

Fig. 1. Visible absorption spectra of living erythrocytes recorded in the oxy, deoxy and met states showing the major visible electronic transition bands and the excitation wavelengths used in this study. The darker vertical line represents the HeNe laser whilst the other vertical dotted lines show the excitation lines generated by the tunable laser.

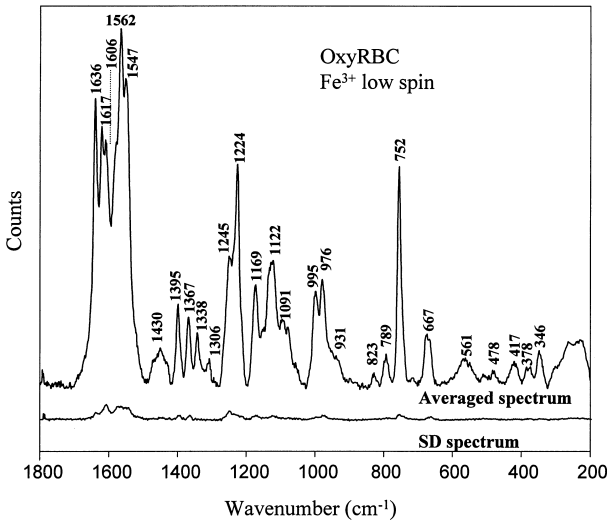

Fig. 2. Averaged and standard deviation Raman spectrum calculated from spectra recorded of 20 single oxyRBCs from a normal human adult in PBS. For each spectrum ten intermittent scans are accumulated with a 10 s laser exposure time. Power at the sample for each spectrum is approx. 1.5 mW.

exhibit profiles characteristic of the respective Hb isolates [27]. The visible spectrum of metRBCs shows the CT band characteristic of high spin haems centred on the excitation wavelength of the HeNe laser. The spectrum of oxyRBCs shows no obvious electronic ground state in the vicinity of the HeNe excitation wavelength. To gain insight into the type of enhancement observed in the spectra of oxyRBCs spectra were recorded in intervals around the Q_0 and CT band of dried oxyRBCs using a tunable laser. The wavelengths investigated are delineated in Fig. 1 and discussed later in the text.

3.2. *Raman microscopy of RBCs and haem isolates with 632.8 nm excitation*

The high concentration of Hb in a single erythrocyte (approx. 22 M) and the relatively long wavelength of the HeNe laser (632.8 nm) has enabled us to record Raman spectra of single living erythrocytes at low power (approx. 1.5 mW) and in a short time span (10 s exposure×10 accumulations). The cell morphology remained totally intact and exhibited no sign of laser scarring after 100 s of intermittent laser exposure and the spectra remained consistent over this time scale. Fig. 2 depicts the averaged spectrum from 20 recorded spectra of different oxyRBCs along with the calculated standard deviation (SD) spectrum. It is clear from the SD spectrum that the variation within a normal RBC population is relatively small with some minor variation in the spin marker band region between 1600–1500 cm^{-1} and the methine deformation region 1300–1200 cm^{-1}. This variation may be attributed to slight variations in Fe spin states between haem moieties within the different cells. The intermittent laser exposure minimised photodissociation and prevented haemolysis in single cells. Fig. 3 illustrates the effect of oxygen photodissociation from crystallised HbA_0 following continuous scanning (100 s) with increasing laser power at 632.8 nm. By increasing the power the

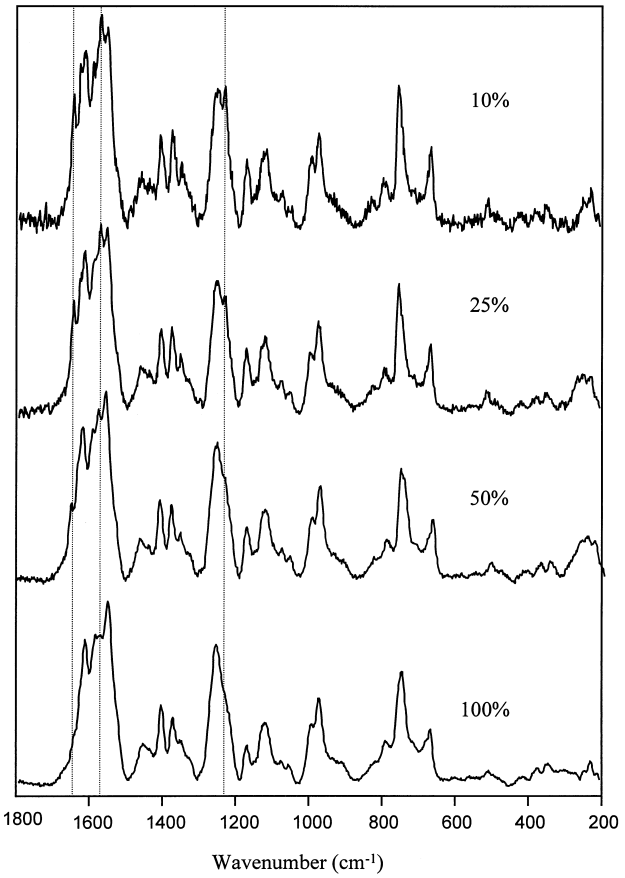

Fig. 3. Power dependence spectra recorded of a single HbA_0 crystal using a HeNe 632.8 nm laser line. At 100% the power is approx. 1.5 mW and for each spectrum ten continuous scans are accumulated with a 10 s laser exposure time. The vertical dotted lines show bands that appear to be power dependent and are thus sensitive to photodissociation of oxygen from the haem.

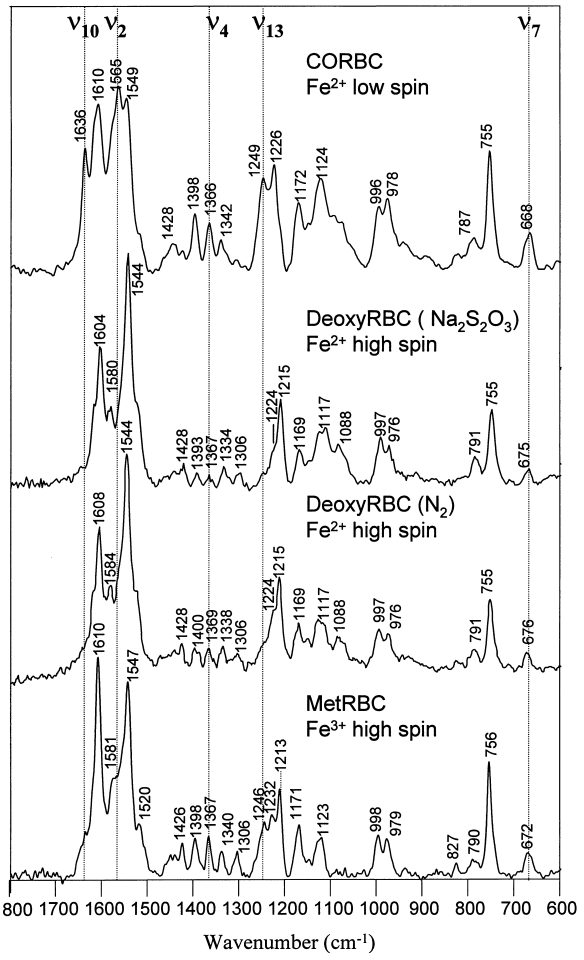

Fig. 4. Raman spectra of a single living erythrocyte in both the oxygenated and deoxygenated states recorded before and after the addition of $Na_2S_2O_4$ and a spectrum of a second cell deoxygenated by equilibrating the RBC suspension with N_2. Spectra of metRBCs and carboxyRBCs are also presented. All spectra are recorded in PBS using the 632.8 nm excitation line generated by a HeNe laser. For each spectrum ten intermittent scans are accumulated with a 10 s laser exposure time. The dashed lines in the spectra indicate bands that disappear following deoxygenation.

low spin marker bands at 1636 (ν_{10}), 1562 (ν_2) and 1224 (ν_{10}) cm^{-1} diminish. Fig. 4 depicts spectra of a single erythrocyte after the addition of $Na_2S_2O_4$ and the spectra of carboxyRBCs and metRBCs. The addition of $Na_2S_2O_4$ to a suspension of erythrocytes causes the oxygen to egress from the cells without diffusion of the dithionite anion through the erythrocyte membrane [28]. To verify that the spectral changes observed upon the addition of $Na_2S_2O_4$ are the result of deoxygenation and not from direct reduction of the haem moieties we saturated an erythrocyte suspension with N_2 and produced an almost identical spectrum. The variation between the two spectra is well within the SD spectrum presented in Fig. 2. The spectrum of a metRBC is similar to that of a deoxyRBC both in terms of wavenumber position and relative intensity. Conversely the spectra of a carboxyRBC and an oxyRBCs are also very similar, especially in the region of the spin state marker bands at 1600–1500 cm^{-1} and methine deformation 1300–1200 cm^{-1} modes. Fig. 5 depicts the spectra of single crystals of haemin, haematin,

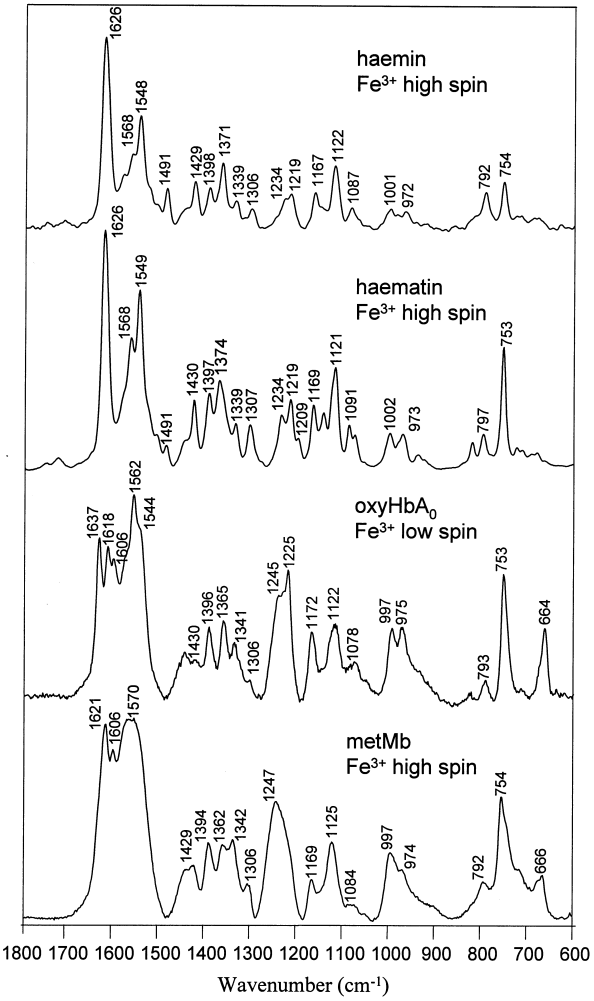

Fig. 5. Raman spectra of single crystals of haemin, haematin, HbA_0, and metHb recorded under similar conditions as the erythrocytes presented in Fig. 4. The spectra clearly show that the majority of bands appearing in the erythrocyte spectra are haem in origin.

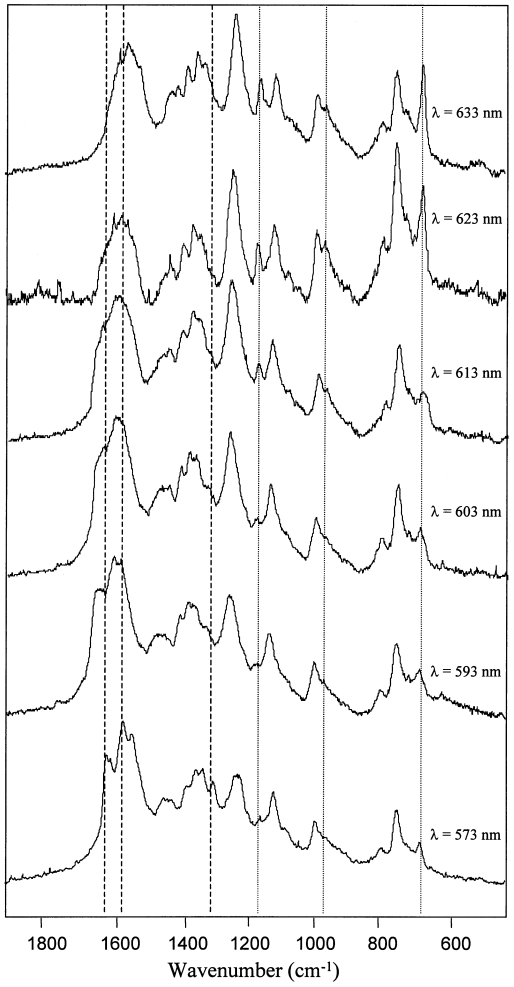

Fig. 6. Spectra recorded at various excitation wavelengths of dried oxyRBCs in the 573–633 nm region using a tunable all line argon-ion laser to pump a rhodamine 6G dye laser. Each spectrum is made up of eight spectral windows and the laser exposure time for each window is 180 s. Between each measurement the laser is calibrated to the 520.5 cm^{-1} silicon band and the power adjusted to approx. 1 mW. Dashed vertical lines highlight the bands that become enhanced approaching the Q_0 electronic transition while dotted vertical lines indicate bands that appear resonance enhanced at approx. 633 nm.

HbA_0 and metMb. The spectra clearly show that the majority of bands observed in the erythrocyte spectra originate from the protein-free Fe-porphyrin. The spectra of haemin and haematin exhibit a number of features similar to those of the high spin haem moieties encapsulated within metRBCs and deoxyRBCs. For example both exhibit the characteristic high spin pattern in the 1650–1500 cm^{-1} region with prominent bands appearing between 1624–1610 cm^{-1}, 1585–1580 cm^{-1} and 1547–1544 cm^{-1}. The doublet at 1245 cm^{-1} and 1224 cm^{-1}, observed in the spectra of low spin haems, appears red shifted in the spectra of haemin and haematin. This shift, however, is not as dramatic as that observed upon deoxygenating erythrocytes.

3.3. Excitation of low spin haem at 573–633 nm, 780 nm and 1064 nm

To gain further insight into the apparent enhancement at 632.8 nm spectra of dehydrated oxyRBCs were recorded in intervals between 573 and 633 nm. Fig. 6 depicts spectra recorded of oxyRBCs at the various excitation wavelengths generated using an argon-ion laser to pump a 6G rhodamine dye laser. The dramatic intensity of the 1245 (ν_{13}-B_{1g}), 1172 (ν_{30}-B_{2g}), 976 (ν_{46}-B_{1g}) and 672 (ν_7-A_{1g}) cm^{-1} bands at 633 nm is indicative of resonance enhancement and shows a mixture of totally symmetric and

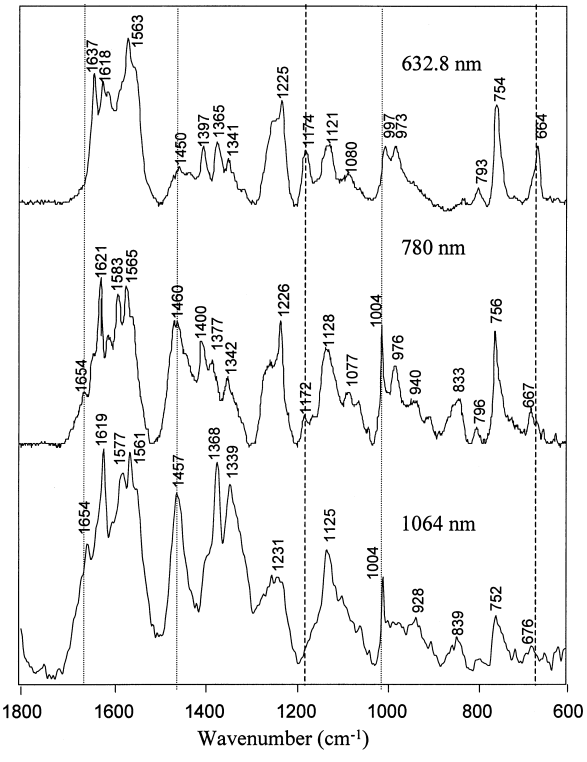

Fig. 7. Spectra recorded of HbS at 632.8 nm, 780 nm and 1064 nm. Spectra are vector normalised and baseline corrected to enable comparison. The dotted lines show bands of proteinaceous origin becoming more enhanced at the longer wavelengths.

Table 1
Observed bands, assignments, local coordinates and symmetry terms for haem moieties observed at 632.8 nm

oxyRBC	deoxyRBC	carboxyRBC	metRBC	Haemin	Haematin	HbA_0	metMb	Mode [17,29]	Local coordinate [29][a]	Symmetry [29][b]
1636 (dp)	absent	1636	1636 w	absent	absent	1637	1636[c]	ν_{10}	$\nu(C_\alpha C_m)_{asym}$	B_{1g}
1617	1618 sh	1618 sh	1617	1626	1626	1618	1621	$\nu(C_a = C_b)$	$\nu(C_a = C_b)$	
1606 (ap)	1606	1610	1610	absent	absent	1606	1606	ν_{19}	$\nu(C_\alpha C_m)_{asym}$	A_{2g}
1582 Sh	1580	1581 sh	1581	1584 sh	1584	1582	1570[c]	ν_{37}	$\nu(C_\alpha C_m)_{asym}$	E_u
1562 (p)	absent	1565	absent	1568	1568	1562	1558[c]	ν_2	$\nu(C_\beta C_\beta)$	A_{1g}
1547 (dp)	1544	1549	1547	1548	1549	1544	1548[c]	ν_{11}	$\nu(C_\beta C_\beta)$	B_{1g}
1430 (dp)	1428	1428	1426	1429	1430	1430	1426	ν_{28}	$\nu(C_\alpha C_m)_{sym}$	B_{2g}
1395 (ap)	1393	1398	1398	1398	1397	1396	1391	ν_{20}	ν(pyr quater-ring)	A_{2g}
1367 (p)	1367	1366	1367	1371	1374	1365	1362	ν_4	$\nu(\text{pyr half-ring})_{sym}$	A_{1g}
1338	1334	1342	1340	1339	1339	1341	1340	ν_{41}	$\nu(\text{pyr half-ring})_{sym}$	E_u
1306 (ap)	1306	1306	1306	1306	1307	1306	1311	ν_{21}	$\delta_{asym}(C_mH)$	A_{2g}
1245	absent	1249	1246 w	absent	absent	1245	1246	ν_{13}	$\delta(C_mH)$	B_{1g}
1224 (dp)	1224[c]	1226	1230	1234	1234	1225	1224[c]	ν_{13} or ν_{42}	$\delta(C_mH)$	B_{1g} or E_u
1210[c] (dp)	1215	1209[c]	1213	1219	1219	1209[c]	1210[c]	ν_{5+} ν_{18}	$\delta(C_mH)$	B_{1g}
1169 (dp)	1169	1172	1171	1167	1169	1172	1170	ν_{30}	$\nu(\text{pyr half-ring})_{asym}$	B_{2g}
1122 (ap)	1117	1124	1123	1122	1121	1122	1125	ν_{22}	$\nu(\text{pyr half-ring})_{asym}$	A_{2g}
1091 (ap)	1088	1089	absent	1087	1091	1078	1084	ν_{23}	$\nu(C_\beta C_1)_{asym}$	A_{2g}
995 (dp)	997	996	998	1001	1002	997	997	ν_{45}	$\nu(C_\beta C_1)_{asym}$	E_u
976 (dp)	976	978	979	972	973	975	974	ν_{46}	$\delta(\text{pyr deform})_{asym}$ and/or $\gamma(=C_bH_2)_{sym}$	E_u
823 (dp)	827	825	827	825	825	828	827	γ_{10}	$\gamma(C_mH)$	B_{1u}
789 (p)	791	787	790	792	797	793	792	ν_6	ν(pyr breathing)	A_{1g}
752 (dp)	755	755	756	754	753	753	754	ν_{15}	ν(pyr breathing)	B_{1g}
667 (p)	676	668	672	absent	absent	664	666	ν_7	$\delta(\text{pyr deform})_{sym}$	A_{1g}

RBC, red blood cell. p, polarised; dp, depolarised; ap, anomalously polarised; ν, stretch; δ, in-plane deformation; γ, out-of-plane deformation; sym, symmetric; asym, asymmetric; pyr, pyrrole; deform, deformation; w, weak band relative to others.

[a]Subscripts refer to haem labelling scheme adopted by Hu et al. [29].

[b]Based on calculated depolarisation ratios for oxyRBC and by comparison with Hu et al. [29].

[c]Only observed after calculating second derivative.

non-totally symmetric vibrational modes. As the wavelength decreases so to does the intensity of these bands. Approaching the Q_0 electronic transition (centred at approx. 580 nm) the bands at 1636 (ν_{10}-B_{1g}), 1582 (ν_{37}-E_u) and 1306 cm^{-1} (ν_{21}-A_{2g}) become enhanced. Consequently the mechanism of enhancement for a number of modes at 633 nm appears to be independent of pre-resonance Raman excitation. Fig. 7 compares spectra recorded of HbS using longer wavelengths (632.8, 780 and 1064 nm). By exciting with 780 nm and 1064 nm the very sharp phenylalanine vibration at 1004 cm^{-1} is observed along with the Amide I mode at 1654–1657 cm^{-1} and CH_2/CH_3 deformation modes associated with aliphatic amino acids at approx. 1460 cm^{-1}. These bands are absent at 632.8 nm excitation. At 780 nm bands at 1621 cm^{-1} (from the $\nu(C_a = C_b)$ of vinyl groups), 1583 (ν_{37}), 1400 (ν_{20}) and 1128 (ν_{22}) appear enhanced while those at 1172 (ν_{30}) and 672 (ν_7) cm^{-1} appear diminished indicating another type of enhancement mechanism for excitation at 780 nm. The intensity of the bands at approx. 1172 (ν_{30}) and 664 (ν_7) cm^{-1} is further reduced at 1064 nm. More surprising is the shift in wavenumber of ν_4 from 1365 cm^{-1} using 632.8 nm to 1377 cm^{-1} with 780 nm excitation indicating a wavenumber dependence on excitation wavelength.

4. Discussion

4.1. Band assignment

Specific band assignments based on polarisation data and by comparison with previous studies [13,17,29] are detailed in Table 1. In the idealised D_{4h} symmetry of metallo-porphyrins the depolarisation ratios for the A_{1g}, B_{1g}, B_{2g} and A_{2g} modes are expected to be 1/8, 3/4, 3/4 and infinity corresponding to polarised (p), depolarised (dp), and anomalously polarised (ap) bands, respectively [29]. However, overlapping vibrational modes and depolarisation dispersion resulting from different excitation wavelengths can result in deviations from these ideal values [30,31]. Consequently, the polarisability and resulting symmetry terms depicted in Table 1 for an oxygenated erythrocyte are based on qualitative values for the depolarisation ratios and the results of previous studies [13,17,29]. For the ease of band assignment and because both oxyRBCs and deoxyRBCs share a number of common bands we have adopted the same labelling notation for both states.

The high wavenumber region (1650–1500 cm^{-1}) of all spectra presented comprises mainly of porphyrin in-plane vibrational modes that are sensitive to porphyrin distortion. In oxyRBCs and carboxyRBCs this region of the spectrum consists of six bands appearing at approx. 1636, 1620–1617 (shoulder in deoxyRBCs), 1610–1606, 1565–1562 and 1549–1547 cm^{-1}. In deoxygenated erythrocytes and met erythrocytes this region comprises three principal bands appearing at 1610–1604 cm^{-1}, 1582–1580 cm^{-1} and 1547–1544 cm^{-1}. The disappearance of the band appearing at approx. 1636 (dp) cm^{-1} assigned to ν_{10} is in good agreement with other Raman studies [1,2,14,16,24] and is indicative of porphyrin doming. The band at 1562 (dp) cm^{-1} (ν_2) in oxygenated erythrocytes vanishes in the deoxygenated and met states, the former in agreement with a recent FT-Raman study [16]. The band at 1617 cm^{-1} in oxyRBCs, assigned to $\nu(C=C)$ of vinyl groups [29], appears as a shoulder feature on the band at approx. 1606 cm^{-1} in deoxyRBCs.

Bands in the central region (1400–1300 cm^{-1}) of the Raman spectra presented are reported to be sensitive to the oxidation and spin state of the central metal atom within the porphyrin macrocycle [2–4,9,10,14–16,26,32,33]. A dramatic result following O_2 egression is the almost complete disappearance of the so-called 'oxidation state marker' band, characteristic of the pyrrole half-ring symmetrical stretching vibration, which appears as a medium intensity polarised band in the spectra of oxyRBCs (1367 cm^{-1}), carboxyRBCs (1366 cm^{-1}), haemin (1371 cm^{-1}), haematin (1374 cm^{-1}), HbA_0 (1365 cm^{-1}) and metRBCs (1368 cm^{-1}). The band appearing at 1397 (ap) cm^{-1} (assigned to ν_{20}) is less intense following O_2 egression, while the band at 1334 cm^{-1} (assigned to ν_{41}) is now the dominant feature of this triplet. These modes along with ν_4 belong to the same coordinate, the pyrrole half-ring symmetrical stretch but with different phasing [29]. Another significant difference is the apparent dramatic shift in wavenumber of the doublet at 1245 cm^{-1} and 1224 cm^{-1} in oxyRBCs which upon deoxygenation shifts

to 1224 cm^{-1} and 1215 cm^{-1}. Second derivative analysis of oxyRBCs revealed the region between 1250 and 1200 cm^{-1} to be comprised of three bands at approx. 1248, 1224 and 1215 cm^{-1} (data not shown). The intense band at approx. 1248 cm^{-1}, which dominates the spectra of the erythrocytes, HbA and metHb appears to shift to 1225 cm^{-1} after the egression of O_2. In the spectra of haemin and haematin a relatively small band is observed at 1234 cm^{-1}. Bands observed between 1230 and 1225 cm^{-1} in RR spectra of metallo-porphyrins are usually assigned to C-H in-plane bending vibrations of the methine hydrogen [2,17,24,29]. Based on the work of Salmaso et al. [13] on the resonance Raman characterising of EPO we assign the 1224 cm^{-1} band to ν_{13} and the band at 1215 cm^{-1} to $\nu_5+\nu_8$. An alternative assignment for the band at 1224 cm^{-1} is ν_{42} of E_u symmetry [29].

It is tempting to assign the 1250–1245 cm^{-1} band appearing in the erythrocyte and apoprotein spectra to the Amide III mode in agreement with a non-resonant Raman study on whole blood [14]. Supporting this assignment is the absence of this band in the protein-free porphyrins and the dramatic shift observed upon deoxygenation. However, the absence of the Amide I mode at approx. 1650 cm^{-1} precludes assignment of this band to the Amide III. Fig. 7 shows that the Amide I mode appears more intense as excitation approaches the longer wavelengths.

The low wavenumber region in the spectra of oxyRBCs are dominated by a number of strong bands at approx. 1169, 1122, 1091, 995, 976, 931, 823, 789, 752 and 667 cm^{-1}, most of which have been previously assigned [29]. While the wavenumber values for oxyRBCs and deoxyRBCs for the above-mentioned bands are generally the same (± 1 cm^{-1}), the relative intensities of some of these bands differ. Bands below 650 cm^{-1} are very small and not considered further in this discussion.

4.2. Structure of the prosthetic group within the cell

The results clearly demonstrate the sensitivity of the technique to haem perturbation in a single living erythrocyte. All high spin domed haems encapsulated in living cells have characteristic high spin bands at approx. 1606 cm^{-1} (ν_{10}), 1581 (ν_{37}), 1547 (ν_{11}), 1224 (ν_{13}) and 1209 ($\nu_5+\nu_8$) cm^{-1} and share some common spectral features with haemin and haematin. Low spin encapsulated haems, like those in oxygenated and carboxyRBCs, appear at approx. 1636 (ν_{10}), 1562 (ν_2), 1249 cm^{-1} (ν_{13}) and 1224 ($\nu_5+\nu_8$) and share features similar to oxyHbA_0. The almost complete disappearance of ν_{10}, ν_2, ν_4, ν_{13} and ν_7 in deoxygenated erythrocytes indicates that the Hb porphyrin macrocycle is more symmetrical in the deoxygenated state than the oxygenated state in single erythrocytes. This is possibly attributed to ruffling effects induced by the translocation of the Fe atom into the porphyrin plane resulting in distortion from the idealised planar D_{4h} symmetry and an increase in non-totally symmetric components. The totally symmetric A_{1g} mode (ν_7) at approx. 672 cm^{-1} in high spin encapsulated haems undergoes a dramatic intensity reduction when converted to low spin haem moieties. This band is very sensitive to excitation wavelength and is also power dependent. The similarity between carboxyRBCs and oxyRBCs spectra is in good agreement with earlier studies comparing carboxyHb and oxyHb [1,2] and supports the low spin state predicted for the Fe atom in carboxyHb.

The observation that (ν_4) appears invariant to oxidation state in living cells is indeed intriguing. The wavenumber value of ν_4 is thought to reflect the electron population in the porphyrin π^* orbitals, with an increasing population weakening the bonds and bringing about a decrease in vibrational wavenumber. The electron population in the π^* orbitals is thought to be increased by back donation of the electrons from the Fe atom's $d\pi$ orbitals. Because back donation is greater for Fe(II) than Fe(III), the oxidation state marker bands are lower in wavenumber compared to those of Fe(II) [33]. The reduced intensity of ν_4 upon deoxygenation in the current study is in agreement with a previous FT-Raman study comparing deoxyHb and oxyHb using 1064 nm excitation [15]. Contrary to a number of other Raman studies on Hb isolates and whole blood [2,4,10,16,34], we observe no shift in this band from the oxy state to the deoxy state. The wavenumber value of ν_4 in the ferric state of Hb is generally reported to vary between 1375 and 1370 cm^{-1} compared to 1360–1350 cm^{-1} in the ferrous state [3,24]. The appearance of ν_4 in the narrow range between 1364 and 1367 cm^{-1} in oxygenated, deoxygenated, carboxylated and metRBCs infers that there is no

correlation between the wavenumber of ν_4 and the oxidation state of the Fe cation, at least in red blood cells using 632.8 nm excitation. The reliability of the correlation of ν_4 as the ferric marker band has been questioned by others [5,35]. Spaulding et al. [5] found ν_4 to be relatively invariant for a wide range of metals despite the large anticipated differences in charge density migration from the various metals to the conjugated porphyrin ring indicating that the charge distribution around the central Fe atom is not a fundamental factor in the positioning of this line. The position of ν_4 in the spectrum of metMb at 1362 cm^{-1} verified on two independent samples of metMb suggests a ferrous oxidation state for the haem Fe in this apoprotein, which is clearly not the case. Consequently, the results are not compatible with the back donation hypothesis as a mechanism to explain the disappearance of ν_4 upon O_2 egression because no red shift of ν_4 is observed. Moreover, the wavenumber value of ν_4 appears to be dependent on excitation wavelength as demonstrated by the 12 cm^{-1} red shift observed going from 632.8 nm to 780 nm excitation.

The molecular environment of the methine vibrations appearing between 1300 and 1200 cm^{-1} would be severely affected by protein interactions and haem-stacking. An early study on metallo-octaethyl porphyrins and haems [2] suggested that the wavenumber of the band appearing at approx. 1220 cm^{-1} is dependent on the strength of the co-ordination between the porphyrin and metal. The decrease in wavenumber from approx. 1225 cm^{-1} in oxyRBCs to approx. 1210 cm^{-1} in deoxyRBCs may reflect such a dependence.

4.3. Enhancement mechanism

The spectra at 632.8 nm are dominated by a mixture of bands both totally symmetric ($\rho < 0.75$) and non-totally symmetric ($\rho \geq 0.75$) indicative of type A and B scattering. Consequently enhancement of some bands around 633 nm could be the result of preresonance Raman scattering as eluded to in early HeNe excitation studies [36,37]. However, non-resonance Raman scattering due to the highly polarisable nature of the haem chromophore and the high concentration of Hb is also a candidate to explain the observed enhancement. Alternatively, resonance enhancement resulting from CT bands in the 600–650 nm region may account for the strong Raman scattering intensities observed in some bands at this wavelength. To gain further insight into this enhancement mechanism we recorded spectra of dehydrated oxyRBCs at intervals between 573 and 633 nm and compared spectra of HbS at 632.8 nm, 780 nm and 1064 nm. The resonant enhancement mechanism for certain Raman vibrational modes (1172 (ν_{30}), 976 (ν_{45}) and 672 (ν_7) cm^{-1}) at 632.8 nm in low spin haems appears not to involve either preresonance excitation from the Q_0 band nor resonant enhancement from the CT band. The absence of an electronic ground state transition at approx. 633 nm in the visible spectrum of living oxyRBCs precludes resonance involving the CT absorption band. Furthermore, the enhanced bands involve different modes compared to those previously reported for a laser excitation study on EPO (high spin ferric haem) in eosinophils where a strong CT absorption band is centred at approx. 633 nm [13]. The spectra of deoxyRBCs and metRBCs show that the majority of bands exhibit similar relative intensities even though their visible absorption profiles are markedly different at 632.8 nm. The result infers that the enhancement is independent of CT resonance. It is only at longer excitation wavelengths (780 and 1064 nm) that the Amide I and phenylalanine bands are observed, although phenylalanine modes have been previously reported from 514 nm excitation [13]. At 780 nm a different set of modes are enhanced and some modes observed at 632.8 nm are dramatically reduced. These results demonstrate the unique nature of band enhancement occurring at 632.8 nm especially in low spin haems. More work is required to elucidate the mechanism of this enhancement, which is the subject of ongoing research in our laboratories.

4.4. Conclusion

We have characterised the R to T state transition in a single living erythrocyte. Domed high spin encapsulated haems can be easily discerned from low spin more planar forms in the spin marker band region (1650–1500 cm^{-1}) and in the methine deformation region (1300–1200 cm^{-1}). Furthermore, we have demonstrated that the enhancement of a number of Raman bands using 633 nm excitation is in-

dependent of both pre-resonance scattering from the Q_0 band and direct resonance from the CT band.

The information gained by in vivo single erythrocyte molecular analysis has important ramifications to the understanding of fundamental erythrocyte processes and may prove useful for diagnosing and monitoring the effect of oxidative stress in erythrocytes. Moreover, one can study the effects of drugs and other treatments designed to increase oxygen affinity in the treatment of such conditions as anaemia and altitude sickness. The methodology will also allow the in vivo investigation of a number of interesting phenomena, for example erythrocyte sickling associated with homozygous sickle cell anaemia, where polymerisation of Hb into fibres upon deoxygenation is thought to occur. We plan to investigate the nature of haem stacking and its association with the reverse sickling phenomenon that characterises the homozygous sickle cell trait. This may provide a molecular insight into the dynamical nature of the 'haem pocket' throughout this extraordinary morphological transition.

Acknowledgements

This work was supported by a grant from Monash University (Faculty of Science) and a Large Australian Research Council Grant. We wish to thank the staff at the Victorian Transplantation and Immunogenetics Service for donating blood samples and general assistance. We also thank Dr Paul Spizziri (School of Physics, Melbourne University) for his time and technical expertise for measurements using the tunable laser and Dr J. Church (Deakin University, Geelong) for his time and assistance for measurements on the FT-Raman instrument.

References

[1] T.C. Streakas, T.G. Spiro, Biochim. Biophys. Acta 263 (1972) 830–833.
[2] H. Brunner, A. Mayer, H. Sussner, J. Mol. Biol. 70 (1972) 153–156.
[3] T.G. Spiro, T.C. Streakas, J. Am. Chem. Soc. 96 (1973) 338–345.
[4] T. Yamamoto, G. Palmer, J. Biol. Chem. 248 (1973) 5211–5213.
[5] L.D. Spaulding, C.C. Chang, N.-T. Yu, R.H. Felton, J. Am. Chem. Soc. 97 (1975) 2517–2525.
[6] T. Kitagawa, Y. Kyogoku, T. Iizuka, M.I. Saito, J. Am. Chem. Soc. 98 (1976) 5169–5173.
[7] J.M. Burke, J.R. Kincaid, S. Peters, R.R. Gagne, J.P. Collman, T.G. Spiro, J. Am. Chem. Soc. 100 (1978) 6083–6088.
[8] T.G. Spiro, in: T.T. Theophanides (Ed.), Infrared and Raman Spectroscopy of Biological Molecules, vol. 43, D. Reidel Publ. Co., Dordrecht, 1979, pp. 267–275.
[9] A. Lanir, N.-T. Yu, R.H. Felton, Biochemistry 18 (1979) 1656–1660.
[10] L. Rimai, I. Salmeen, D.H. Petering, Biochemistry 14 (1975) 378–382.
[11] G. Smulevich, F. Neri, M.P. Marzocchi, K.G. Welinder, Biochemistry 35 (1996) 10576–10585.
[12] G. Smulevich, Biospectroscopy 4 (1998) S3–S17.
[13] B.L.N. Salmaso, G.J. Pupells, P.J. Caspors, R. Floris, R. Wever, J. Greve, Biophys. J. 67 (1994) 436–446.
[14] Y. Ozaki, A. Mizuno, H. Sato, K. Kawauchi, S. Muraishi, Appl. Spectrosc. 46 (1992) 533–536.
[15] T. Johjima, H. Wariishi, H. Tanaka, Biochem. Bioiphys. Res. Commun. 226 (1996) 601–606.
[16] B. Venkatesh, S. Ramasamy, M. Mylrajan, R. Asokan, P.T. Manoharan, J.M. Rifkind, Spectrochim. Acta A 55A (1999) 1691–1697.
[17] M. Abe, T. Kitagawa, K. Kyogoku, J. Chem. Phys. 69 (1978) 4526–4534.
[18] J.J. Weiss, Nature 202 (1962) 83–84.
[19] C. Balagopalakrishna, P.T. Manoharan, O.O. Abugo, J.M. Rifkind, Biochemistry 35 (1996) 6393–6398.
[20] S. Franzen, J.C. Lambry, B. Bohn, C. Poyart, J.L. Martin, Nat. Struct. Biol. 1 (1994) 230–233.
[21] C. Piffat, D. Melamed, T.G. Spiro, J. Phys. Chem. 97 (1993) 7441–7450.
[22] C. Otto, N.M. Sijtsema, J. Greve, Eur. Biophys. J. 27 (1998) 582–589.
[23] P. Jeannesson, J.F. Angiboust, J.C. Jardillier, M. Manfait, in: IEEE Eighth Annual Conference of the Engineering in Medicine and Biology Society, Fort Worth, TX, 1986, p. 1404.
[24] C.W. Ong, Z.X. Shen, K.K.H. Ang, U.A.K. Kara, S.H. Tang, Appl. Spectrosc. 53 (1999) 1097–1101.
[25] G.J. Puppels, J.H.F. Olminkhof, G.M.J. Segers-Nolten, C. Otto, F.F.M. Mul de, J. Greve, Exp. Cell Res. 195 (1991) 361–367.
[26] T.G. Spiro, J.D. Stong, P. Stein, J. Am. Chem. Soc. 101 (1979) 2648–2655.
[27] W.G. Zijlstra, A. Buursma, O.W. van Assendelft, Visible and Near Infrared Absorption Spectra of Human and Animal Haemoglobin Determination and Application, VSP, Utrecht, 2000.
[28] J.A. Sirs, Biochim. Biophys. Acta 126 (1966) 28–36.
[29] S. Hu, K.M. Smith, T.G. Spiro, J. Am. Chem. Soc. 118 (1996) 12638–12646.
[30] S. Hu, T.G. Spiro, J. Phys. Chem. 99 (1995) 7193–7194.

[31] R. Schweitzer-Stenner, W.J. Dreybrodt, J. Raman Spectrosc. 23 (1992) 539–550.
[32] R.H. Felton, in: D. Dolphin (Ed.), The Porphyrins, Physical Chemistry, Part A, vol. III, Academic Press, New York, 1978, pp. 347–393.
[33] P.R. Carey, Biochemical Applications of Raman and Resonance Raman Spectroscopies, Academic Press, London, 1982.
[34] T.G. Spiro, J.M. Burke, J. Am. Chem. Soc. 98 (1976) 5482–5489.
[35] A. Szabo, L.D. Barron, J. Am. Chem. Soc. 97 (1975) 660–662.
[36] H. Buerger, H. Burczyk, J.W. Buchler, J.H. Fuhrhop, F. Hofler, B. Schrader, Inorg. Nucl. Chem. Lett. 6 (1970) 171–174.
[37] K.N. Solovyov, N.M. Ksenofontova, S.F. Shkirman, T.F. Kachura, Spec. Lett. 6 (1973) 455–467.